GEOGRAFICKÝ ČASOPIS / GEOGRAPHICAL JOURNAL 78 (2026) 4, 207-218
DOI: https://doi.org/10.31577/geogrcas.2026.78.4.02

INSTITUTE OF GEOGRAPHY SLOVAK ACADEMY OF SCIENCES

Geografický časopis
Geographical Journal

Microclimatic interaction in semi-humid environments: Quantification of the urban heat island, shading efficiency, and their impact on the humidex heat stress index. Case study: Souk Ahras City, Algeria

Fatma Khelifa[1,*], Imed Eddine Khelfa[2], Djamel Alkama[1]

[1] Department of Architecture, Faculty of Sciences and Technology, Guelma, Algeria, khelifatma0@gmail.com, alkama.djamel@univ-guejma.dz
[2] Department of Architecture, Faculty of Architecture and Urbanism, Polytechnic School of Architecture and Urbanism (EPAU), Algiers, Algeria, imad14000@hotmail.com
* Corresponding author

Abstract

The urban heat island degrades public health and outdoor thermal comfort by exacerbating extreme heat conditions within urban environments, especially during heat waves. This study examines these effects and shading effectiveness in Souk Ahras using a tripartite geographic gradient (rural, suburban, and urban) to evaluate both urban and intra-urban thermal impacts. Specifically, the study quantifies the urban heat island intensity by calculating the diurnal temperature differences through a rigorous in situ approach, while assessing the Humidex heat stress index at sunny and shaded locations. The results indicate that the peak intensity of the urban heat island was recorded at 14:00. At this hour, the urban heat island intensity, calculated relative to the rural station, reached 3.7 °C, while the intra-urban urban heat island showed an average maximum temperature difference of 2.0 °C. This confirms that Souk Ahras is affected by the urban heat island phenomenon, which has a quantifiable effect on outdoor thermal comfort. Based on the difference in Humidex values of 5.1 points between locations A and B, and 3.46 points between locations C and D, tree shade is an effective strategy for reducing heat stress and enhancing outdoor thermal comfort.

Key words:
urban heat island, intra-urban heat island, humidex index, Souk Ahras, outdoor thermal comfort, heat stress, shading efficiency, tripartite geographic gradient

1 INTRODUCTION

The notion of climate change refers to a long-lasting alteration in the climate's features, which can be caused by manmade changes in land use and atmospheric composition, natural internal processes, or external natural forces (Paula et al., 2025). Rising levels of carbon dioxide and other greenhouse gases in the atmosphere are key contributors to climate change, which has resulted in an increase in Earth's surface temperature and has significantly influenced other climatic factors. Consequently, urban residents are anticipated to be particularly exposed to the increased thermal risks, which may also have an impact on human health, given current climatic trends (Mohammad Harmay & Choi, 2023).

As anthropogenic climate change intensifies, it is anticipated that the observed trends of heat waves will persist and accelerate in almost all urbanized regions (Domeisen et al., 2023). Furthermore, cities often have warmer air than the surrounding suburban and rural areas, especially at night. This phenomenon is known as the urban heat island (UHI) effect (Wang et al., 2025); it poses health concerns and can exacerbate heat stress (Kim et al., 2024).

Many studies have demonstrated the synergistic interaction between UHI and heat waves (Ward et al., 2016; Ramamurthy & Bou-Zeid, 2017; Wei et al., 2022; Luo et al., 2023; Cheval et al., 2024; Joshi et al., 2024; Xue et al., 2024).

Numerous direct and indirect effects of the UHI on cities and their residents include increased energy use for air conditioning and a rise in heat-related deaths and illnesses, especially for vulnerable populations. These effects would be more pronounced during heat waves (Kong et al., 2021), which are defined by the Heat Wave Duration Index (HWDI) as times when the daily maximum temperatures are at least 5 °C higher than the seasonal average for at least five days in a row (Frich et al., 2002).

The UHI effect is becoming one of the major issues affecting human health and the urban environment. Thus, one of the most prevalent and challenging topics in contemporary urban thermal environment research is evaluating the impact of the UHI effect on outdoor thermal comfort (OTC) and the strategies to reduce UHI effects (Qaid et al., 2016; Aram et al., 2020; Ren et al., 2023).

Several studies have shown that OTC is strongly impacted by the UHI effect (Salman & Saleem, 2021; Tabatabaei & Fayaz, 2023; Behzad & Guilandoust, 2024; Li, Y., et al., 2025; Zhou et al., 2025).

The general definition of thermal comfort is the state of mind that conveys contentment with the thermal surroundings (Hensen, 1990). The complexity of studying OTC is significantly higher than that of indoor environments because of the greater instability of temperature and humidity changes, the difficulty of controlling radiation heat and wind speed in the outdoor

environment, and the greater variation in human metabolic rate. Heat-related illnesses like heat rash, heat cramps, heat stroke, and even death have been linked to high outdoor temperatures (Ren et al., 2023).

OTC is a key concept in creating sustainable and healthy urban environments. Reducing stress can improve the quality of life and psychological well-being of city dwellers (Ogce et al., 2025). Mitigating the UHI effect is one of the most crucial steps in enhancing OTC. Urban vegetation, particularly trees, is now the most successful of the many techniques that experts have suggested to lessen this effect (Gomaa et al., 2025).

In addition to having a significant impact on the micrometeorological conditions in their immediate area, urban trees help alleviate pedestrians , thermal stress in high temperatures. This is mostly because tree canopies alter the local radiation balance, especially by shading the person‘s body and the surrounding ground or constructed surfaces, and the improvement of evapotranspiration (Massetti et al., 2019; Vatani et al., 2024).

Several previous studies have used various relevant thermal indices to calculate heat stress during periods of high heat and its effects on human thermal comfort (Karimi et al., 2023; Kotharkar et al., 2024; Kotharkar & Dongarsane, 2024; Mahdavinejad et al., 2024; Pantavou et al., 2025; Su et al., 2026).

While complex biometeorological indices are widely used, such as Physiological Equivalent Temperature (PET) and Universal Thermal Climate Index (UTCI), simpler ones, including Humidex heat stress index (HX), remain important tools for public health warnings and preliminary estimations for specific climates. Building on this, the present study aims to assess the combined impact of the UHI and shading efficacy on OTC during heat waves in the city of Souk Ahras. To achieve this, the research employs a tripartite geographic gradient (rural, suburban, and urban), specifically selecting Independence Square and the April 16 Esplanade for detailed analysis. The methodology focuses on computing and evaluating the HX index at various points to quantify the effectiveness of local mitigation strategies.

2 MATERIAL AND METHODS

Geographical Context and Specific Features of the Local Climate

The Souk Ahras region is located in northeastern Algeria at an elevation of 697 meters (36°17‘11“N, 7°57‘4“E). It extends along Algeria‘s border, forming a natural link between Tunisia and the rest of the country. The Souk Ahras region covers an area of 4,359.65 km². Geographically, Souk Ahras sits in a basin surrounded by complex mountainous terrain (500 to 1,400 m) that is part of the Tell Atlas in the north and the High Plains in the south (Fig. 1). This mountainous region is quite high in the north and slightly lower in the south of the region. In the north, it is divided into two alignments by the Medjerda Valley, with a general northeast/southwest direction.

Due to its location at the summit of the Tellian Atlas, Souk Ahras region has a dual climate that is primarily defined by temperature and precipitation. The High Plains in the south have a continental climate with desert inclinations, while the northern part of the region has a Mediterranean climate (see Fig. 2).

Specifically, the northern zone receives an average annual rainfall of 650 mm, whereas the southern plains range between 350 and 600 mm. The thermal profile is marked by an average annual temperature of 15.6 °C; winters are rigorous with January temperatures between 1 °C and 15 °C (23 to 47 frost days per year), while summers are hot and dry with July and August maximums typically ranging from 25 °C to 35 °C.

Experimental Device and rural, suburban, and urban Gradient

The research methodology employs a multi-scale comparative approach. At the urban scale, the intensity of the UHI in Souk Ahras is quantified using a tripartite geographic gradient (rural, suburban, and urban).

This setup allows for the evaluation of two distinct

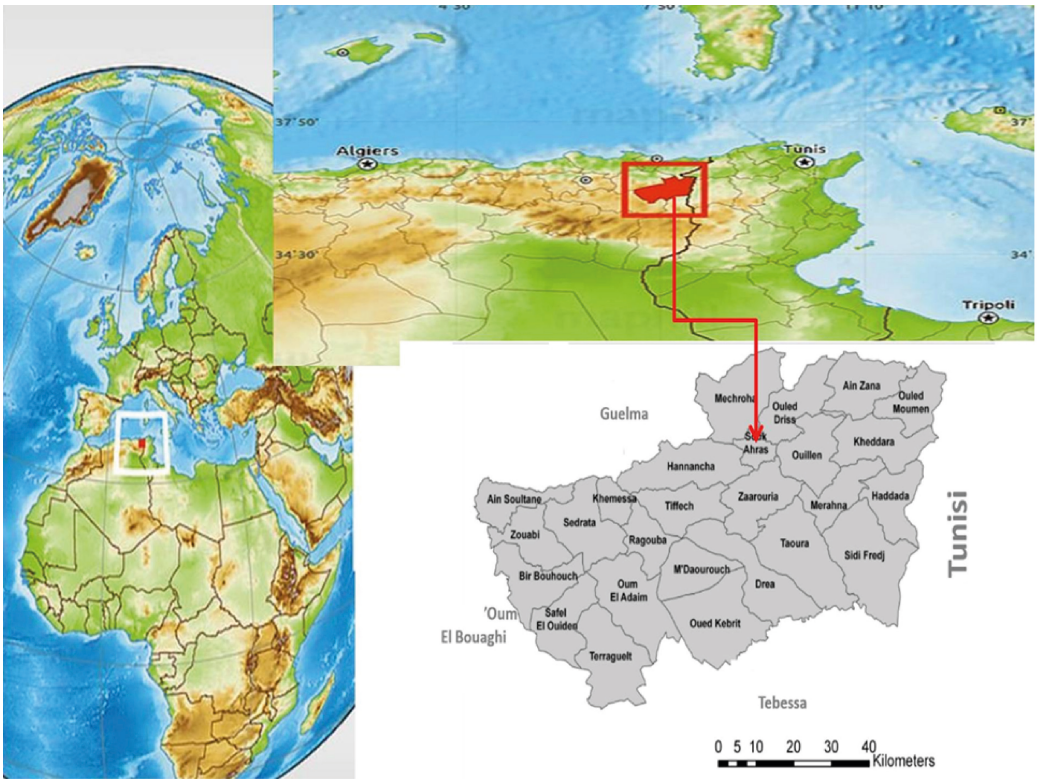


Fig. 1. Geolocation of the region of Souk Ahras

Source: (Boukehili et al., 2018)

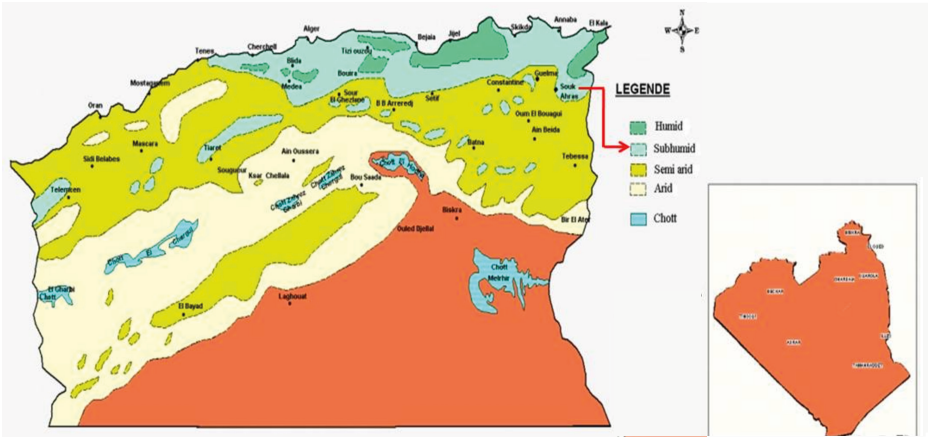


Fig. 2. Bioclimatic map of Algeria
Source: Adapted from the Bioclimatic Map of Algeria, National Agency for Spatial Planning (ANAT), Algiers, 2004

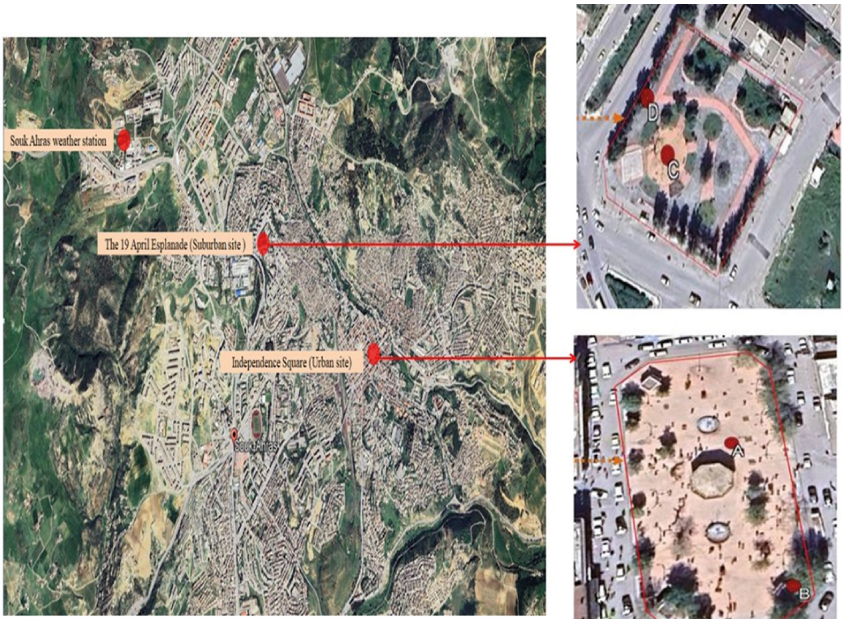


Fig. 3. Location and experimental measurement of microclimate acquisition points
Source: Base map: © Google Earth/Maxar (2024), modified by authors

phenomena: the UHI (urban vs. rural reference) and the intra-urban UHI (urban vs. suburban gradient).

At the micro-climatic scale, these two public spaces were selected to evaluate the impact of vegetation on pedestrian Outdoor Thermal Comfort. By calculating the HX at both sun-exposed points and points shaded by trees, the study aims to demonstrate the crucial role of tree canopy shade in mitigating thermal stress and improving the local microclimate (see Fig. 3).

To support the comparative analysis, three distinct sites were selected along the geographic gradient, each representing a specific urban morphology:

- The rural reference station 60423: (36° 17‘ 51.02“ N, 7° 55‘ 22.10“ E) – located at the city‘s periphery, this site serves as the thermal baseline. It is characterized by open land, minimal construction, and natural soil, reflecting the regional climate without urban interference (Fig. 4).
- The urban site: Independence Square (36° 17‘ 5.30“ N, 7° 57‘ 22.98“ E) – located in the dense historical heart of Souk Ahras, this site is defined by high building density and preponderance of mineral surfaces, narrow streets, and intense human activity (see Fig. 5), resulting in a low sky view factor, which is favorable for maximal UHI intensity. Points were selected to compare full solar exposure (point A) against natural shade (point B), highlighting the impact of urban density on pedestrian comfort.
- The suburban site: 19 April Esplanade (36° 17‘ 28.32“, 7° 56‘ 25.80“ E) – situated as a transition zone, this space features moderate building density and significant vegetation cover (see Fig. 6). Within this site, measurements were taken at a sun-exposed point (Point C) and a shaded point (Point D) under tree canopies. This setup allows for a precise comparison of tree shade efficacy within a baseline temperature setting, contrasting with the more densely built urban environment.

Instrumentation and Data Acquisition Protocol

A series of measurements related to microclimatic conditions was collected in Souk Ahras for three days during the hottest days of that summer (July 16-18, 2022). Microclimatic measurements were made using an experimental protocol consisting of two different but synchronized measurement types:

- In-situ measurements: Mobile readings were performed simultaneously at four urban locations (A, B, C, and D). These points were strategically paired to compare sun-exposed and shaded environments under tree canopies. Measurements were taken at a standard height of 1.50 m using a Chauvin Arnoux C.A 846 thermo-hygrometer

to measure the air temperature (Ta) and relative humidity (RH) as shown in Figure 7. At each point, a 3-minute stabilization period was observed, and the sensor was protected by a portable radiation shield to eliminate solar bias; while wind speed (Va) was determined using a Trotec B16 anemometer

- Regional reference: Meteorological data (air temperature, relative humidity, and wind speed) were based on the records of the Souk Ahras weather station (60423) at two-hour intervals. These data serve as the rural baseline for quantifying the UHI intensity.

Between measurement cycles, the handheld devices were systematically stored in a cool, shaded environment to prevent thermal inertia. By synchronizing the station's records with the in-situ measurements, the study establishes a rigorous framework for evaluating both the UHI magnitude and HX variations.

Data Processing and Quantification of Thermal Indices

Quantification of the Urban Heat Island (ΔT_{UHI})

The UHI intensity was determined by calculating the air temperature differences between the representative sites along the geographic gradient (Stewart & Oke, 2012). Measurements and records were made using a two-hour interval from 06:00 to 18:00 (local time) over three days to provide detailed observation of temporal variations in temperature during the day.

To isolate the impact of urbanization, two levels of UHI were quantified using the average values from the three-day campaign:

- UHI (ΔT_{UHI}): Calculated as the difference between the urban sunny location (T_A) and the rural reference temperature from the Souk Ahras weather station (T_{Rural}):

$$\triangle T_{UHI} = T_A - T_{Rural} \quad (1)$$



Fig. 4. Souk Ahras weather station (Station 60423)
Source: Base map: © Google Earth/Maxar (2024), modified by authors (2025)



Fig. 5. Composition of the Independence Square views
Source: authors´photos (2025)

- Intra-urban UHI ($\Delta T_{UHI-Intra}$): Calculated as the difference between the urban sunny location (T_A) and the suburban sunny location (T_C)

$$\triangle T_{UHI-Intra} = T_A - T_C \quad (2)$$

All temperatures used for these calculations correspond to sun-exposed conditions at each site to ensure atmospheric consistency. This dual-scale quantification makes it possible to separate the general impact of the city's climate from the specific variations caused by local urban density and morphology.

Evaluation of Thermal Comfort using Humidex

By calculating the HX at each of the four measurement locations during the three days of measurements, the amount of thermal stress experienced by the pedestrians has been assessed. The HX is an empirical heat stress index originally introduced by the researchers Masterton and Richardson to evaluate human thermal discomfort felt by the general population under different air temperature and humidity conditions.

HX is expressed as a linear combination of air temperature and water vapor pressure (Diaconescu et al., 2023). This index was calculated for each of the seven daily readings taken over the three days, and then averaged to obtain a statistically more reliable daily heat stress curve. The formula used to calculate the HX is as follows:

$$HX = T_a + h \quad (3)$$

where T_a is the air temperature in degrees Celsius, and h is the humidity factor, calculated by:

$$h = 0.5555 \times (p - 10.0) \quad (4)$$

where p represents the water vapor pressure expressed in kilopascals (kPa). The calculated HX values have been interpreted using the standard scale used by Météo Canada in order to categorize the degree of stress experienced at various measurement points (Lukić, 2019) as summarized in Table 1.

Quantification of Microclimatic Mitigation

To assess the effectiveness of the shade provided by existing trees at each intervention site (Independence Square or the 16 April Esplanade), we directly compared the average HX values of measurements taken during the study period from 6:00 to 18:00 in sunny areas (A and C) and shaded areas (B and D). From the difference obtained, two indicators were determined: urban attenuation ($HX_A - HX_B$) and suburban attenuation ($HX_C - HX_D$).

The significance of these differences was statistically validated, demonstrating that the reduction in heat stress provided by shade is a consistent phenomenon across both morphological contexts.

3 RESULTS

Table 2 shows extreme values of air temperature (Ta), relative humidity (RH), and wind speed (V_a) recorded at the four study points over the three days of measurements. To provide a comprehensive thermal baseline, the table also includes synchronized data from the rural meteorological station (60423). These data allow us to analyze the intensity of the UHI (by comparing A with the rural station) and the intra-urban UHI (by comparing A and C), as well as the effect of shading (by comparing A with B and C with D).“

Analysis of microclimatic data

Figure 8 presents a parallel comparison of the three parameters measured across the study area, focusing on four specific points within the two intervention sites, urban (Points A and B) and suburban (Points C and D), compared against the rural reference station (60423) from 06:00 to 18:00.

The thermal analysis reveals significant microclimatic variations between the urban and suburban sites and the regional baseline (Station 60423).

The peak average temperature (T_a) was recorded at 14:00 at Point A (Urban, Sunny), reaching 40.2 °C, whereas the rural reference station peaked at a lower value of 36.5 °C. Simultaneously, Point D (Suburban, Shady) demonstrated the highest cooling potential, recording the lowest afternoon temperature of 34.03 °C.

Regarding the early morning values at 06:00, the rural station recorded a minimum of 24.7 °C, while the lowest temperatures within the intervention sites were 26.5 °C at Point B (Urban, Shady) and 27.16 °C at Point D (Suburban, Shady).

Concerning relative humidity (RH), the rural reference station maintained the highest baseline



Fig. 6. Composition of the suburban site views – 19 April Esplanade
Source: authors´photos (2025)



Fig. 7. In situ data acquisition instruments used for microclimatic surveys: (left) Thermo hygrometer (Chauvin Arnoux C.A 846) for Ta and RH, and (right) Propeller anemometer (Trotec B16) for wind speed (Va)
Source: authors´photos (2025)

Tab. 1. Interpretation scale for the Humidex (HX) and classification of thermal comfort levels and associated risks

Range of Humidex		Degree of comfort
<29	Comfortable	A little discomfort and fatigue with prolonged physical activity is possible
30–39	Some discomfort	Exhaustion due to heat is possible with prolonged physical activity
40–44	Great discomfort	Avoid strenuous physical activity, possible heat cramps, or heat exhaustion
45–54	Dangerous	Prolonged physical activity can lead to heat stroke
>55	Very dangerous	A heat stroke is unavoidable if physical activity continues

Sources: Baum et al., (2009)

(48% at 06:00). Within the sites, the highest value was recorded at 06:00 at the shaded urban location (Point B) at 40.26%. By 14:00, a convergence in dryness was observed between the sun-exposed points (A and C) at approximately 22.7%, significantly lower than the rural station‘s 28.5%.

Finally, wind speed (Va) reflected the impact of urban density and site morphology. While the rural station reached 2.50 ms-1, the open suburban site (Point D) recorded a maximum of 1.37 ms-1, whereas the dense urban core (Point A) saw the lowest ventilation at 0.6 ms-1 (at 06:00) and 0.93 ms-1 (at 14:00).

Urban Heat Island Quantification (ΔTUHI): Diurnal Cycle and Average Intensity

The thermal divergence between the intervention sites and the rural reference station (60423) was calculated in order to quantify the intensity of the UHI. The diurnal cycle of ΔT_{UHI} reveals that the urban microclimate is consistently warmer than its rural counterpart, though the intensity fluctuates significantly throughout the day.

To precisely evaluate this phenomenon, two indicators were analyzed: UHI (ΔT_{UHI}) and intra-urban UHI ($\Delta T_{UHI\text{-}Intra}$). The data in Table 2 show that the average maximum temperature at Point A (Urban, Sunny) reached 40.2 °C, while the regional baseline peaked at 36.5 °C and 38.2 °C at Point C (Suburban, Sunny). Consequently, at 14:00, the peak intensities were recorded as: ΔT_{UHI} = 3.7 °C, $\Delta T_{UHI\text{-}Intra}$ = 2.0 °C.

As illustrated in Figure 9, the temperature remains high with a ΔT_{UHI} consistently exceeding 3 °C from 06:00 to 18:00. Although the intra-urban intensity of 2.0 °C at peak hours is considered to be in the low-to-medium range, the global intensity of 3.7 °C confirms a substantial thermal decoupling between the city of Souk Ahras and its rural surroundings.

The fact that maximum temperatures can exceed 40 °C at the study sites during the period reveals how important these heat islands are in escalating urban heat stress and its detrimental consequences on thermal comfort and human health.

Statistical Validation of the UHI Intensity

In order to assess the significance of the temperature differences observed, a paired Student‘s t-test was performed to compare the urban data set (point A) with that of the rural reference station. This statistical approach is crucial in determining whether the temperature contrast is a constant phenomenon or the result of random climatic fluctuations.

The analysis yielded a p-value of 5.06×10-5 ($p < 0.001$), which is significantly lower than the standard threshold of 0.05. This result provides strong evidence that the temperature difference between the urban core and the rural surroundings is statistically highly significant.

The April 16 Esplanade, which represents the suburban site, was excluded from this specific validation in order to focus on the maximum intensity of the urban heat island. This binary comparison provides a clearer signal of the thermal contrast between urban and rural areas, as evidenced by the high R2 (0.96) obtained from the linear regression (see Fig. 10).

This strong correlation indicates that 96% of the temperature variation in the urban area is directly explained by the regional climatic signal, while the constant offset (intercept) reflects the persistent intensity of the Urban Heat Island. These metrics ($p < 0.001$ and R2 = 0.96) validate the reliability of the measurement network and the representativeness of the findings for Souk Ahras.

Tab. 2. Summary of Average Microclimatic Extremes (16–18 July 2022)

Points Site / Exposition		meteorological station (60423	A Urban, sunny	B Urban, shady	C Suburban, sunny	D Suburban, shady
Ta_{max}	°C	36.5	40.2	36.83	38.2	34.03
$t(Ta_{max})$	h	14:00	14:00	14:00	14:00	14:00
Ta_{min}	°C	24.7	27.2	26.5	27.5	27.16
$t(Ta_{min})$	h	6:00	6:00	6:00	6:00	6:00
RH_{max}	%	48.2	40.26	40.6	38.13	35.9
$t(RH_{max})$	h	6:00	6:00	6:00	6:00	6:00
RH_{min}	%	28.5	22.7	23.36	22.66	21.53
$t(RH_{min})$	h	14:00	14:00	14:00	14:00	14:00
Va_{max}	ms^{-1}	1.55	0.93	1.24	1.37	1.76
$t(Va_{max})$	h	18:00	18:00	12:00	12:00	8:00
Va_{min}	ms^{-1}	1.10	0.6	0.70	0.65	0.89
$t(Va_{min})$	h	6:00	6:00	6:00	6:00	6:00

Sources: authors' (2025)

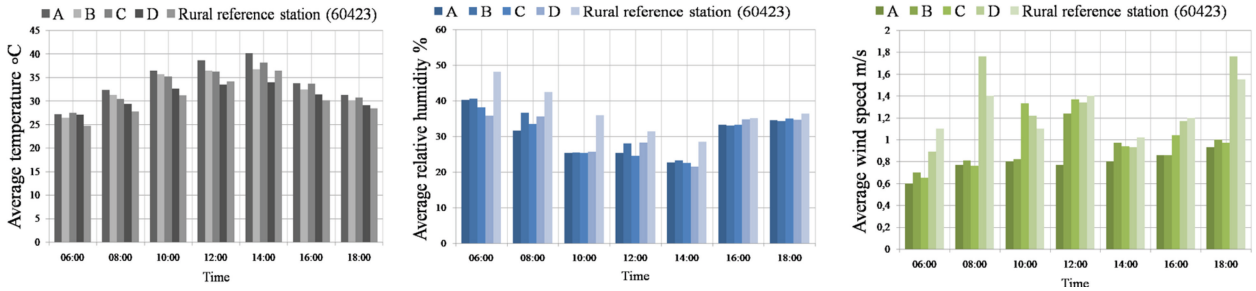


Fig. 8. The average of current microclimatic data measured at the intervention sites during the study period
Source: authors' (2025)

Evaluation of the effect of shading on outdoor thermal comfort: the Humidex

In order to quantify the real impact of microclimatic changes on user comfort, we employed the HX calculated by (3) and (4). This index is important because it models the thermal stress experienced by combining the air temperature (Ta) and the humidity factor (h).

We applied these formulae to all our data for the four measurement points (A, B, C, D) in order to identify areas of intense heat stress and accurately assess the reduction in heat sensation provided by shade.

Analysis of the HX confirms that perceived heat stress reached critical levels during the study period. At Point A (Urban, Sunny), the average maximum HX (HXmax) was 45.12 at 14:00, placing this area in the 'dangerous category' according to the standard scale, indicating a major health risk for users of this public space during prolonged physical activity. These signs warn of potential heatstroke (Masitoh & Rusydi, 2020).

As illustrated in Figure 11, the shade provided by trees in urban areas (point B) is an essential mitigation measure, reducing the HX_{max} to 40.02 at 14:00.

With an estimated difference of ΔHX_{max} = 5.1, this reduction lowers the perceived level from the 'Great discomfort' category to the 'Some discomfort' category, representing a significant gain in terms of comfort and safety during the day.

The impact of tree shade is amply demonstrated in suburban (C vs. D) when the average HX_{max} drops from 40.63 to 37.17 at 14:00, marking a difference of ΔHX_{max} = 3.46. This significant gain enables the perception of the category «Great discomfort» (C) at the category «Some discomfort» (D).

Figure 12 illustrates the diurnal evolution of the average values calculated for HX index at the four points during the study period. The analysis of the diurnal cycle of the HX for the four curves shows a slow rise starting in the morning, reaching a peak at all sites between 12:00 and 16:00.

The persistence of the UHI is demonstrated by a more thorough examination of the Diurnal Cycle, which shows that the perception of temperature difference between the sunny urban area (A) and the shaded suburban area (D) is significant over the course of the measurement period.

This difference between the two extremes is most noticeable at 14:00, when it reaches its maximum, ΔHX_{max} = 7.95 (between 45.12 and 37.17), and it never completely disappears.

The curve for the shaded suburban point (D) has a constant vertical offset but a profile resembling that of (C).

This deviation reaches its maximum at 3.46 HX points (between HX_{maxc} = 40.63 and HX_{maxD} = 37.17), demonstrating at each two-hour interval how tree shade effectively mitigates heat stress and enhances pedestrians' thermal comfort.

Nonetheless, although the reduction effect of shade was most potent in the suburban setting, it was still important in the urban context. The same reduction in heat stress was observed by comparing the sunny urban point (A) and shaded urban point (B), which achieves 5.1 HX points.

Shading effectiveness is systematically evaluated using urban and reference ΔHX_{max} mitigation indicators, and the results show that maximal effectiveness typically coincides with the afternoon peak of heat stress (see Tab. 3).

Tab. 3. Comparison of Maximum Shading Effectiveness (ΔHXmax) between Urban and Reference Environments

Indicator	Calculation	Results
$\Delta HXmax_{urban}$	45.12 (A) – 40.02 (B)	5.1 HX points
$\Delta HXmax_{reference}$	40.63 (C) – 37.17 (D)	3.46 HX points

Source: authors´ (2025)

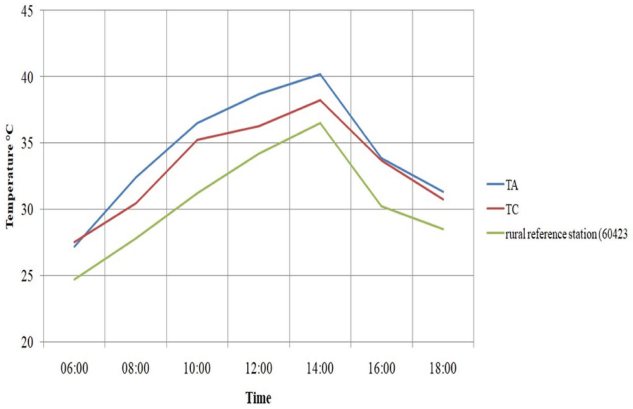


Fig. 9. Average daily temperature cycles for urban, suburban, and rural reference sites during the measurement period
Source: authors´ (2025)

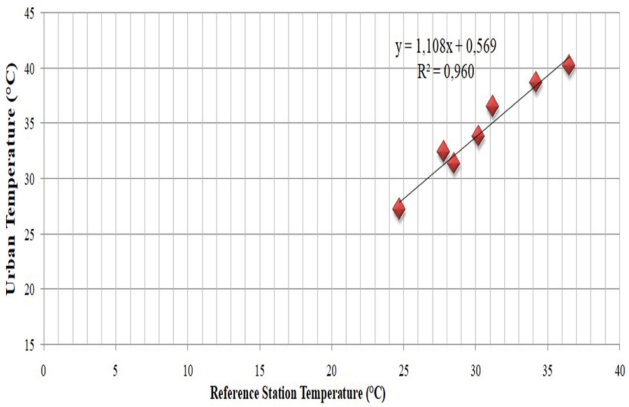


Fig. 10. Linear regression and correlation analysis between the rural reference station and the urban core (Point A)
Source: authors´ (2025)

4 DISCUSSIONS

Factors influencing the Urban Heat Island's intensification

Based on the results obtained from the Quantification of UHI, this phenomenon does not occur only at a specific time, and its intensity can vary considerably throughout the day (Al-Obaidi et al., 2021).

Impact of Surface Albedo on Urban Heat Retention

One of the main causes of the increase in air temperature Ta recorded during the day, from 6:00 to 18:00, is the use of mineralized materials, which often have low albedo, struggle to rapidly release the thermal energy they collect from the sun, and retain heat. Albedo is the ability of a surface to reflect incident solar radiation, and it is measured on a scale from 0 to 1, which represents reflectivity and total absorption, respectively (Elgendy et al., 2025).

In the visible spectrum, dark colors are responsible for low albedo or high absorptivity, while lighter colors have high albedo, synonymous with high reflectivity of solar radiation (Lopez-Cabeza et al., 2022).

Consequently, the use of light-colored materials, as seen in the Souk Ahras city center, results in a decrease in absorption in the visual spectrum (see Fig.13).

Although the absorption of the infrared portion of the light is mostly independent of color perception, the value of reflectivity is primarily determined by the color and rugosity of the material. As a result, numerous studies have examined the effects of pavement material colors on surface temperature and sensible heat generation, as indicated in several studies (Santamouris, 2013; T. Zhang et al., 2025).

Geographical and Anthropogenic Drivers

It should be highlighted that a city's specific geographic features, climate, and seasonal variations, anthropogenic heat emissions, and changes in soil cover in this region have also a significant impact on the UHI effect (Mohajerani et al., 2017; Roshan et al., 2022).

Urban Morphology and Ecological Alteration Factors

The intensity of urban heat island effect obtained during the study period, with a UHI (ΔTUHI) of 3.7 °C and an intra-urban UHI (ΔTUHI-Intra) of 2.0 °C, shows the existence of persistent heat overload brought on by urbanization, which has a quantifiable impact on the warmth seen in this region and may worsen the UHI effect due to pollution levels, energy consumption and the decrease in vegetation (Krüger et al., 2024; Saikia et al., 2024).

Vegetation Cover and Microclimatic Regulation Factors

In the city center of Souk Ahras, the built environment is gradually replacing the natural vegetative cover; this reduction in the percentage of vegetation immediately results in a warming effect that impacts the urban thermal environment and urban ecosystems. Urban vegetation can preserve urban microclimates because trees have been shown to provide shade and evapotranspiration, which cool cities. However, trees might influence urban aerodynamic roughness and wind flow, which may restrict heat dissipation (Gatto et al., 2020; Meili et al., 2021).

Thermal Exposure and Public Health Stress Factors

The maximum temperatures measured at the study sites, reaching 40 °C, demonstrate the severity of urban heat stress and the exacerbation of the UHI effect. Heat stress can also have a significant impact on the daily activities of users of these public spaces, as excessive exposure to heat during daily activities can have adverse effects on physical health (Arifwidodo & Chandrasiri, 2020).

The OTC of users is therefore strongly influenced by the UHI effect due to the high outdoor temperatures and humidity levels recorded (Cheela et al., 2021). Improving thermal comfort and effectively reducing heat stress in public spaces are now crucial factors in raising users' quality of life. Using and incorporating vegetation is one of the best ways to mitigate the negative effects of urban heat islands (Binabid & Anteet, 2024; Safavi-Gerdini et al., 2025; Zhao et al., 2025).

Tree shade as a natural strategy for mitigating heat stress and improving outdoor thermal comfort

Results from the HX analysis at the intervention points revealed that tree shade mitigates maximum HX values, reducing them by 5.1 points at sites A and B, and by 3.46 points at sites C and D. This uniformity across different measurement sites suggests that shade is the primary factor in lowering heat stress.

Therefore, by lowering air temperature, raising relative humidity, moderating wind speed, reducing irradiation, and consequently decreasing the heat absorption of artificial surfaces (Huang et al., 2020; Zhang, L., et al., 2020; Aleksandrowicz & Pearlmutter, 2023), the installation of shade has greatly reduced heat stress at these locations.

Analysis of the HX diurnal cycle for the four points shows that the HX peak in all sites is obtained between 12:00 and 16:00. Confirming that the peak of thermal stress occurs when the air temperature and radiant heat

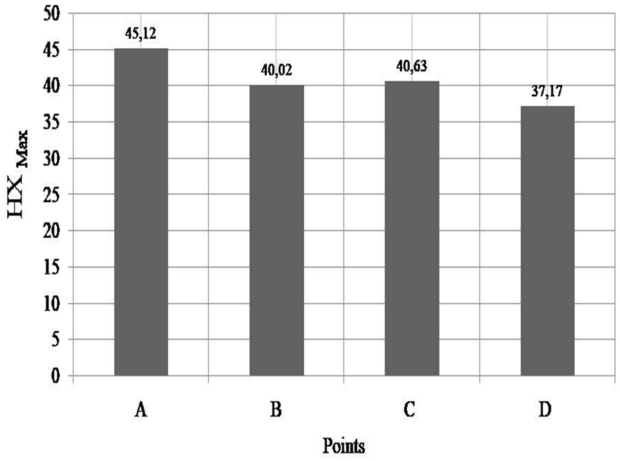


Fig. 11. Maximum Humidex (HX_{max}) recorded at urban and suburban sites
Source: authors´ (2025)

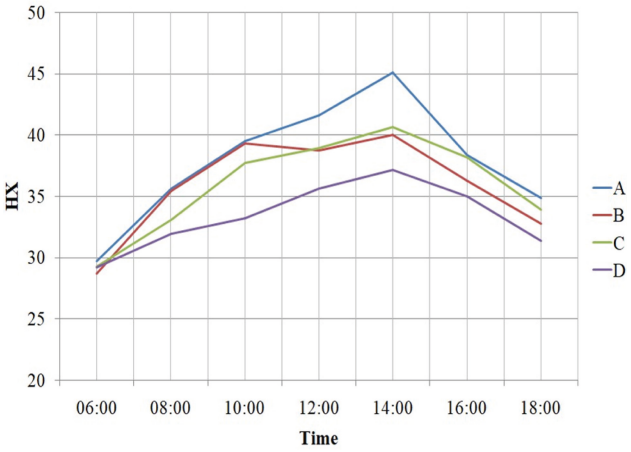


Fig. 12. Average HX diurnal cycle for the four measurement points (A, B, C, D)
Source: authors´ (2025)

accrual are highest and moisture content is also at a high water vapor pressure causing the peak in the combined effects of heat and humidity (Fang et al., 2026).

The UHI effect remained well established throughout the study period. The difference in perceived temperature between the sunny urban area A and the shaded suburban area D was highest around 14:00 with a maximum HX difference ΔHXmax = 7.95 points, and did not completely disappear after that time, demonstrating that the effects of the UHI are a constant occurrence (Li, D., et al., 2024; Liu et al., 2024). This suggests that the intensity of the surrounding UHI has only a slight impact on the cooling and insulating capabilities of shade devices (Cheela et al., 2021; Marando et al., 2022; Zhu & Kensek, 2024).

Trees' natural shade can efficiently block short-wave solar radiation, lowering the heat load on pedestrians. Thus, the mean radiant temperature (Tmrt) is mostly influenced by shading (Kántor et al., 2018; Qiu et al., 2025).

Additionally, it also improves their thermal conditions, returning them to a state of neutrality and eliminating the feeling of excessive heat or discomfort (Terrani et al., 2024). The main ways that trees affect microclimates are through transpiration, radiative interactions, and roughness effects. By converting solar radiation and ambient energy into latent heat through transpiration, leaves lower the air temperature and raise the relative humidity (X. Zhang et al., 2025).

5 CONCLUSIONS

During the hottest month of the year, July 2022, in Souk Ahras, a multi-scale comparative approach was employed using a tripartite geographic gradient (rural, suburban, and urban). Specifically, two public spaces and four distinct points were selected for detailed analysis

In order to assess the combined effect of the urban heat island (UHI) and the effectiveness of shading on outdoor thermal comfort, in particular by calculating and analyzing the HX at different locations, a series of measurements relating to three climatic factors were carried out from July 16 to 18, 2022: air temperature (Ta), relative humidity (RH) and wind speed (Va). The findings we obtained quantitatively show that:

- During the warmer months, air temperature (Ta) and relative humidity (RH) play a major role in determining OTC.
- The high temperatures observed during the study period, which can exceed 40 °C, demonstrate the extent to which these urban heat islands exacerbate urban heat stress and its detrimental effects on human health and thermal comfort.
- The UHI does not occur at just one specific time, and its intensity can vary considerably depending on the time of day.
- The UHI effect can be increased by a number of factors, including low-albedo mineralized materials,



Fig. 13. The use of light-colored materials to control solar radiation in the Souk Ahras city center
Source: authors´photos (2025)

city-specific geographic features, climate, and seasonal variations, anthropogenic heat emissions, changes in land cover, urbanization, and, lastly, a decrease in vegetation cover.

- Due to the high recorded outdoor temperatures and humidity levels, the UHI effect has a significant impact on users' outdoor thermal comfort.
- Peak HX values can be reduced by the shade that trees give; Because shade lowers air temperature (Ta), increases relative humidity (RH), moderates wind speed (Va), lowers irradiation, and ultimately reduces heat absorption by artificial surfaces, it is the main factor in minimizing heat stress.
- The research also confirms the effectiveness of the integration of trees into public spaces to mitigate heat stress, which is a significant problem in urban environments. Although trees theoretically affect the microclimate through transpiration and surface roughness, the results of the research emphasize the importance of the effect of trees on the radiative interaction and the provision of shade. The direct effect of the tree canopy on the thermal stress perceived by users is the reduction of the HX values recorded on shaded sites compared to the sites exposed to the sun.

Acknowledgements

Funding: This research did not receive any specific grant from funding agencies in the public, commercial, or not-for-profit sectors.

REFERENCES

Aleksandrowicz, O., & Pearlmutter, D. (2023). The significance of shade provision in reducing street-level summer heat stress in a hot Mediterranean climate. Landscape and Urban Planning, 229, 104588. https://doi.org/10.1016/j.landurbplan.2022.104588

Al-Obaidi, I., Rayburg, S., Półrolniczak, M., & Neave, M. (2021). Assessing the Impact of wind conditions on urban heat islands in large Australian cities. Journal of Ecological Engineering, 22(11), 1–15. https://doi.org/10.12911/22998993/142967

Aram, F., Solgi, E., Garcia, E. H., & Mosavi, A. (2020). Urban heat resilience at the time of global warming: evaluating the impact of the urban parks on outdoor thermal comfort. Environmental Sciences Europe, 32(1), 117. https://doi.org/10.1186/s12302-020-00393-8

Arifwidodo, S. D., & Chandrasiri, O. (2020). Urban heat stress and human health in Bangkok, Thailand. Environmental Research, 185, 109398. https://doi.org/10.1016/j.envres.2020.109398

Baum, S., Horton, S., Low Choy, D., & Gleeson, B. (2009). Climate change, health impacts and urban adaptability: Case study of Gold Coast City (Research Monograph No. 11). Urban Research Program, Griffith University.

Behzad, Z., & Guilandoust, A. (2024). Enhancing outdoor thermal comfort in a historic site in a hot dry climate (Case study: Naghsh-e-Jahan Square, Isfahan). Sustainable Cities and Society, 102, 105209. https://doi.org/10.1016/j.scs.2024.105209

Binabid, J., & Anteet, Q. (2024). Numerical study of vegetation effects on thermal comfort for voutdoor spaces at a public school in hot and arid climate. Environmental Advances, 15, 100482. https://doi.org/10.1016/j.envadv.2023.100482

Boukehili, K., Boutabia, L., Telailia, S., Menaa, M., Tlidjane, A., Maazi, M. C., Chefrour, A., Saheb, M., & Véla, E. (2018). Orchidaceae of Souk-Ahras Province (Northeastern Algeria): Inventory, ecology, distribution and conservation issues. Revue d'Écologie (La Terre et La Vie), 73(2), 167–179. https://doi.org/10.3406/revec.2018.192

Cheela, V. R. S., John, M., Biswas, W., & Sarker, P. (2021). Combating urban heat island effect—A Review of reflective pavements and tree shading strategies. Buildings, 11(3), 93. https://doi.org/10.3390/buildings11030093

Cheval, S., Amihăesei, V.-A., Chitu, Z., Dumitrescu, A., Falcescu, V., Iraşoc, A., Micu, D. M., Mihulet, E., Ontel, I., Paraschiv, M.-G., & Tudose, N. C. (2024). A systematic review of urban heat island and heat waves research (1991–2022). Climate Risk Management, 44, 100603. https://doi.org/10.1016/j.crm.2024.100603

Diaconescu, E., Sankare, H., Chow, K., Murdock, T. Q., & Cannon, A. J. (2023). A short note on the use of daily climate data to calculate Humidex heat-stress indices. International Journal of Climatology, 43(2), 837–849. https://doi.org/10.1002/joc.7833

Domeisen, D. I. V., Eltahir, E. A. B., Fischer, E. M., Knutti, R., Perkins-Kirkpatrick, S. E., Schär, C., Seneviratne, S. I., Weisheimer, A., & Wernli, H. (2023). Prediction and projection of heatwaves. Nature Reviews Earth & Environment, 4(1), 36–50. https://doi.org/10.1038/s43017-022-00371-z

Elgendy, D., Tolba, O. & Kamel, T. (2025). The impact of increasing urban surface albedo on outdoor air and surface temperatures during summer in newly developed areas. Scientific Reports, 15(1), 25165. https://doi.org/10.1038/s41598-025-08574-2

Fang, Z., Wu, Z., Feng, X., & Yang, J. (2026). Evaluating combined thermal mitigation strategies and personal protective equipment in hot-humid regions: impacts on outdoor thermal environment and physiological-thermal response. Building and Environment, 288, 113933. https://doi.org/10.1016/j.buildenv.2025.113933

Frich, P., Alexander, L., Della-Marta, P., Gleason, B., Haylock, M., Klein Tank, A., & Peterson, T. (2002). Observed coherent changes in climatic extremes during the second half of the twentieth century. Climate Research, 19, 193–212. https://doi.org/10.3354/cr019193

Gatto, E., Buccolieri, R., Aarrevaara, E., Ippolito, F., Emmanuel, R., Perronace, L., & Santiago, J. L. (2020). Impact of urban vegetation on outdoor thermal comfort: comparison between a mediterranean city (Lecce, Italy) and a northern european city (Lahti, Finland). Forests, 11(2), 228. https://doi.org/10.3390/f11020228

Gomaa, M. M., Nabil, J., Berkouk, D., & Ragab, A. (2025). A comparative study of vegetation strategies for outdoor thermal Comfort in high- and low-density urban areas. Urban Science, 9(10), 416. https://doi.org/10.3390/urbansci9100416

Hensen, J. L. M. (1990). Literature review on thermal comfort in transient conditions. Building and Environment, 25(4), 309–316. https://doi.org/10.1016/0360-1323(90)90004-B

Huang, Z., Wu, C., Teng, M., & Lin, Y. (2020). Impacts of tree canopy cover on microclimate and human thermal comfort in a shallow street canyon in Wuhan, China. Atmosphere, 11(6), 588. https://doi.org/10.3390/atmos11060588

Joshi, K., Khan, A., Anand, P., & Sen, J. (2024). Understanding the synergy between heat waves and the built environment: a three-decade systematic review informing policies for mitigating urban heat island in cities. Sustainable Earth Reviews, 7(1), 25. https://doi.org/10.1186/s42055-024-00094-7

Kántor, N., Chen, L., & Gál, C. V. (2018). Human-biometeorological significance of shading in urban public spaces—Summertime measurements in Pécs, Hungary. Landscape and Urban Planning, 170, 241–255. https://doi.org/10.1016/j.landurbplan.2017.09.030

Karimi, A., Bayat, A., Mohammadzadeh, N., Mohajerani, M., & Yeganeh, M. (2023). Microclimatic analysis of outdoor thermal comfort of high-rise buildings with different configurations in Tehran: Insights from field surveys and thermal comfort indices. Building and Environment, 240, 110445. https://doi.org/10.1016/j.buildenv.2023.110445

Kim, D.-H., Park, K., Baik, J.-J., Jin, H.-G., & Han, B.-S. (2024). Contrasting interactions of urban heat islands with dry and moist heat waves and their implications for urban heat stress. Urban Climate, 56, 102050. https://doi.org/10.1016/j.uclim.2024.102050

Kong, J., Zhao, Y., Carmeliet, J., & Lei, C. (2021). Urban heat island and its interaction with heatwaves: A review of studies on mesoscale. Sustainability, 13(19), 10923. https://doi.org/10.3390/su131910923

Kotharkar, R. & Dongarsane, P. (2024). Investigating outdoor thermal comfort variations across Local Climate Zones in Nagpur, India, using ENVI-met. Building and Environment, 249, 111122. https://doi.org/10.1016/j.buildenv.2023.111122

Kotharkar, R., Dongarsane, P. & Ghosh, A. (2024). Quantification of summertime thermal stress and PET range in a tropical Indian city. Urban Climate, 53, 101758. https://doi.org/10.1016/j.uclim.2023.101758

Krüger, E., Gobo, J. P. A., Tejas, G. T., Souza, R. M. S., Neto, J. B. F., Pereira, G., Mendes, D., & Di Napoli, C. (2024). The impact of urbanization on heat stress in Brazil: A multi-city study. Urban Climate, 53, 101827. https://doi.org/10.1016/j.uclim.2024.101827

Li, D., Wang, L., Liao, W., Sun, T., Katul, G., Bou-Zeid, E., & Maronga, B. (2024). Persistent urban heat. Science Advances, 10(15), eadj7398. https://doi.org/10.1126/sciadv.adj7398

Li, Y., Fei, W., Yang, M., Wang, Y., Du, Y., & Wang, Y. (2025). How to realize large-scale outdoor thermal comfort studies? A systematic review based on OTC characterization, methods and research trends. Frontiers in Sustainable Cities, 7, 1552994. https://doi.org/10.3389/frsc.2025.1552994

Liu, C., Lu, S., Tian, J., Yin, L., Wang, L., & Zheng, W. (2024). Research overview on urban heat islands driven by computational intelligence. Land, 13(12), 2176. https://doi.org/10.3390/land13122176

Lopez-Cabeza, V. P., Alzate-Gaviria, S., Diz-Mellado, E., Rivera-Gomez, C., & Galan-Marin, C. (2022). Albedo influence on the microclimate and thermal comfort of courtyards under Mediterranean hot summer climate conditions. Sustainable Cities and Society, 81, 103872. https://doi.org/10.1016/j.scs.2022.103872

Lukić, M. (2019). An analysis of the influence of air temperature and humidity on outdoor thermal comfort in Belgrade (Serbia) using a simple heat index. Archives for Technical Sciences, 2(21), 75–84. https://doi.org/10.7251/afts.2019.1121.075L

Luo, F., Yang, Y., Zong, L., & Bi, X. (2023). The interactions between urban heat island and heat waves amplify urban warming in Guangzhou, China: Roles of urban ventilation and local climate zones. Frontiers in Environmental Science, 11, 1084473. https://doi.org/10.3389/fenvs.2023.1084473

Mahdavinejad, M., Shaeri, J., Nezami, A., & Goharian, A. (2024). Comparing universal thermal climate index (UTCI) with selected thermal indices to evaluate outdoor thermal comfort in traditional courtyards with BWh climate. Urban Climate, 54, 101839. https://doi.org/10.1016/j.uclim.2024.101839

Marando, F., Heris, M. P., Zulian, G., Udías, A., Mentaschi, L., Chrysoulakis, N., Parastatidis, D., & Maes, J. (2022). Urban heat island mitigation by green infrastructure in European Functional Urban Areas. Sustainable Cities and Society, 77, 103564. https://doi.org/10.1016/j.scs.2021.103564

Masitoh, F., & Rusydi, A. N. (2020). Climatological human comfort using heat and humidity index (Humidex) in Gadingkulon, Malang. IOP Conference Series: Earth and Environmental Science, 412, 012026. https://doi.org/10.1088/1755-1315/412/1/012026

Massetti, L., Petralli, M., Napoli, M., Brandani, G., Orlandini, S., & Pearlmutter, D. (2019). Effects of deciduous shade trees on surface temperature and pedestrian thermal stress during summer and autumn. International Journal of Biometeorology, 63(4), 467–479. https://doi.org/10.1007/s00484-019-01678-1

Meili, N., Manoli, G., Burlando, P., Carmeliet, J., Chow, W. T. L., Coutts, A. M., Roth, M., Velasco, E., Vivoni, E. R., & Fatichi, S. (2021). Tree effects on urban microclimate: Diurnal, seasonal, and climatic temperature differences explained by separating radiation, evapotranspiration, and roughness effects. Urban Forestry & Urban Greening, 58, 126970. https://doi.org/10.1016/j.ufug.2020.126970

Mohajerani, A., Bakaric, J., & Jeffrey-Bailey, T. (2017). The urban heat island effect, its causes, and mitigation, with reference to the thermal properties of asphalt concrete. Journal of Environmental Management, 197, 522–538. https://doi.org/10.1016/j.jenvman.2017.03.095

Mohammad Harmay, N. S., & Choi, M. (2023). The urban heat island and thermal heat stress correlate with climate dynamics and energy budget variations in multiple urban environments. Sustainable Cities and Society, 91, 104422. https://doi.org/10.1016/j.scs.2023.104422

Ogce, S., Ogce, H., Yu, S., & Brown, R. D. (2025). The interaction between urban heat island and urban parks: An in-situ measurement-based review. Land Use Policy, 157, 107628. https://doi.org/10.1016/j.landusepol.2025.107628

Pantavou, K., Kotroni, V., Lagouvardos, K., & Kyriakou, P. (2025). Future changes of bioclimate in Greece: Variations in thermal stress according to the Universal Thermal Climate Index (UTCI). Science of The Total Environment, 980, 179514. https://doi.org/10.1016/j.scitotenv.2025.179514

Paula, D. C. J. D., Valin Jr., M. D. O., Santos, F. M. D. M., Novais, J. W. Z., Ventura, T. M., & Souza, N. S. (2025). The effects of urban morphology in a city with a tropical continental climate in the context of heat islands. Urban Climate, 61, 102381. https://doi.org/10.1016/j.uclim.2025.102381

Qaid, A., Bin Lamit, H., Ossen, D. R., & Raja Shahminan, R. N. (2016). Urban heat island and thermal comfort conditions at micro-climate scale in a tropical planned city. Energy and Buildings, 133, 577–595. https://doi.org/10.1016/j.enbuild.2016.10.006

Qiu, L., Ma, H., Yuan, H., & Chen, H. (2025). Quantify the shading effects on alleviating human thermal stress across different local climate zones in the Yangtze River Delta. Building and Environment, 282, 113249. https://doi.org/10.1016/j.buildenv.2025.113249

Ramamurthy, P. & Bou-Zeid, E. (2017). Heatwaves and urban heat islands: A comparative analysis of multiple cities. Journal of Geophysical Research: Atmospheres, 122(1), 168–178. https://doi.org/10.1002/2016JD025357

Ren, J., Shi, K., Li, Z., Kong, X., & Zhou, H. (2023). A review on the impacts of urban heat islands on outdoor thermal comfort. Buildings, 13(6), 1368. https://doi.org/10.3390/buildings13061368

Roshan, G., Sarli, R., & Fitchett, J. M. (2022). Urban heat island and thermal comfort of Esfahan City (Iran) during COVID-19 lockdown. Journal of Cleaner Production, 352, 131498. https://doi.org/10.1016/j.jclepro.2022.131498

Safavi-Gerdini, A., Shafaat, A., Adib, M., & Norouzian-Maleki, S. (2025). Enhancing outdoor thermal comfort through diverse vegetation, materials, and water bodies: A case study of Fath-Abad Garden in Kerman, Iran. Sustainable Cities and Society, 133, 106844. https://doi.org/10.1016/j.scs.2025.106844

Saikia, P., War, P., Umlong, L. M., & Nath, B. (2024). Impact of urbanization on urban heat island dynamics in Shillong city, India using Google Earth Engine and CA-Markov modeling. Remote Sensing, 16(17), 3212. https://doi.org/10.3390/rs16173212

Salman, A. M., & Saleem, Y. M. (2021). The effect of urban heat island mitigation strategies on outdoor human thermal comfort in the city of Baghdad. Frontiers of Architectural Research, 10(4), 838–856. https://doi.org/10.1016/j.foar.2021.07.002

Santamouris, M. (2013). Using cool pavements as a mitigation strategy to fight urban heat island—A review of the actual developments. Renewable and Sustainable Energy Reviews, 26, 224–240. https://doi.org/10.1016/j.rser.2013.05.047

Stewart, I. D., & Oke, T. R. (2012). Local climate zones for urban temperature studies. Bulletin of the American Meteorological Society, 93(12), 1879–1900. https://doi.org/10.1175/BAMS-D-11-00019.1

Su, Y., Sun, J., Li, S., Li, J., Wu, Z., Li, J., Li, X., Wang, D., & Wang, W. (2026). UTCI assessment of outdoor thermal comfort in arid-hot university campuses during summer. Energy and Buildings, 351, 116683. https://doi.org/10.1016/j.enbuild.2025.116683

Tabatabaei, S. S., & Fayaz, R. (2023). The effect of facade materials and coatings on urban heat island mitigation and outdoor thermal comfort in hot semi-arid climate. Building and Environment, 243, 110701. https://doi.org/10.1016/j.buildenv.2023.110701

Terrani, E., Picción, A., Bentancur, O., & Cruz, G. (2024). Effect of street trees shade on perceived thermal comfort in a south temperate climate: The sidewalks of Montevideo (Uruguay). Heliyon, 10(12), e32762. https://doi.org/10.1016/j.heliyon.2024.e32762

Vatani, M., Kiani, K., Mahdavinejad, M., & Georgescu, M. (2024). Evaluating the effects of different tree species on enhancing outdoor thermal comfort in a post-industrial landscape. Environmental Research Letters, 19(6), 064051. https://doi.org/10.1088/1748-9326/ad49b7

Wang, F., Aldama-Campino, A., Belušić, D., Amorim, J. H., Ribeiro, I., Wiréhn, L., Segersson, D., Döscher, R., Navarra, C., Neset, T.-S., & Lind, P. (2025). Interactions of urban heat islands and heat waves in Swedish cities under present and future climates. Urban Climate, 59, 102286. https://doi.org/10.1016/j.uclim.2025.102286

Ward, K., Lauf, S., Kleinschmit, B., & Endlicher, W. (2016). Heat waves and urban heat islands in Europe: A review of relevant drivers. Science of The Total Environment, 569–570, 527–539. https://doi.org/10.1016/j.scitotenv.2016.06.119

Wei, C., Chen, W., Lu, Y., Blaschke, T., Peng, J., & Xue, D. (2022). Synergies between urban heat island and urban heat wave effects in 9 global mega-regions from 2003 to 2020. Remote Sensing, 14(1), 70. https://doi.org/10.3390/rs14010070

Xue, L., Doan, Q.-V., Kusaka, H., He, C., & Chen, F. (2024). Insights into urban heat island and heat waves synergies revealed by a land-surface-physics-based Downscaling method. Journal of Geophysical Research: Atmospheres, 129(13), e2023JD040531. https://doi.org/10.1029/2023JD040531

Zhang, L., Wei, D., Hou, Y., Du, J., Liu, Z., Zhang, G., & Shi, L. (2020). Outdoor thermal comfort of urban park—A Case Study. Sustainability, 12(5), 1961. https://doi.org/10.3390/su12051961

Zhang, T., Fu, X., Qi, F., Shen, Y., Xu, P., Tao, Y., Liu, T., & Song, Y. (2025). Optimizing pedestrian thermal comfort in urban street canyons for summer and winter: Tree planting or low-albedo pavements? Sustainable Cities and Society, 120, 106143. https://doi.org/10.1016/j.scs.2025.106143

Zhang, X., Ren, P., Yao, L.-Y., Li, Q., Zhong, X., Liu, K.-X., Guo, T.-Y., Yang, J.-H., Zhao, L.-H., Pauleit, S., & Rahman, M. A. (2025). Investigating tree shading and thermal variations in a subtropical zone: single tree to Urban squares. Building and Environment, 283, 113408. https://doi.org/10.1016/j.buildenv.2025.113408

Zhao, Y., Li, R., Niu, J., Shi, X., & Gao, N. (2025). Impact of vegetated facades on microclimate and outdoor thermal comfort across different building morphologies. Building and Environment, 285, 113614. https://doi.org/10.1016/j.buildenv.2025.113614

Zhou, W., Jia, S., & Wang, Y. (2025). Greenery for regulating outdoor thermal comfort in various urban environments of a humid-subtropical climate under extreme heat conditions. Urban Forestry & Urban Greening, 113, 129038. https://doi.org/10.1016/j.ufug.2025.129038

Zhu, Y., & Kensek, K.M. (2024). Mitigating the urban heat island effect: the thermal performance of shade-tree planting in downtown Los Angeles. Sustainability, 16(20), 8768. https://doi.org/10.3390/su16208768



Article first received: 24 November 2025
Article accepted: 14 April 2026